International Journal of Renewable Energy Resources 7 (2017) 8-14

PERMANENT MAGNET SWITCHED FLUX MOTOR TORQUE CAPABILITY: A RELIABLE SOLUTION TO FUELESS VEHICLE APPLICATION

Enwelum I. Mbadiwe and Erwan Sulaiman*
Research Center for Applied Electromagnetics, Faculty of Electrical and Power Engineering,
Universiti Tun Hussein Onn Malaysia, 86400, Parit Raja, Batu Pahat, Johor Malaysia.
Email address: mb.fkee.uthm@gmail.com

ABSTRACT
Electric motor powered by electricity for electric vehicle propulsion is a reliable component now that manufacturing of combustion engine remains complicated and fossil oil, it uses is expensive and getting depleted. This paper presents and analyses a three-phase permanent magnet segmented outer rotor switched flux brushless A.C motor in terms of electromagnetic performances which includes phase flux linkage, cogging torque, induced EMF waveforms, torque-current characteristics and electromagnetic torque for high torque applications. The proposed outer rotor motor consists of 24/10 stator-rotor segments and embracing four set of armature windings with alternate magnet in radial direction. The performance is predicted by 2-D FEA using JMAG Software version 14. Compared with conventional synchronous permanent magnet synchronous motor and hybrid excitation switched flux motor, the proposed motor exhibited high peak magnetic flux linkage, low cogging torque and higher average torque capable of sustaining acceleration for long distance travels. However, it is likely to saturate as the current is increased due to higher armature current, thus will require high magnetic loading for torque capability higher than the conventional machines.

Keywords: Electric vehicle; switched flux motor; segmented rotor; outer rotor; PM excitation**.**

1. INTRODUCTION

Currently, automobile industries are embracing a world-wide competitive market due to demand of vehicles independent of combustion engine for propulsion as economic imperative is becoming full of challenges (Ahmad et al. 2012, Byeong-Mun et al. 2010). However, suitable electric motors demand the following performance characteristics; low costs, high reliability, long life cycle, low acoustic noise, high average torque, constant power during entire speed operation, integrated protection functions and high efficiency (Chen et al. 2010, Enwelum et al. 2018, Fei et al. 2009). As a result of these qualities, automotive motors are undergoing a transition from permanent magnet brushless dc motors and possibly other types of advanced alternating current motors (Galea et al. 2012, Hoang et al. 1997, Hwang et al. 2006). Obviously, permanent magnet machines have been used in electric vehicle technology and performance has greatly improved in less heat loss, less use of energy, increased precision and torque effectiveness for various applications (Jin et al. 2009, Kun et al. 2018).

Switched Flux Machine (SFM) is a stator permanent machine whose rotor is passive as all active materials are contained in the stator only. Based on the flux switching, the stator tooth flux switches its polarity by following the motion of rotor, it operates with double frequency. SFM has three internal excitation kinds such as; current carrying coil excitation (WFSFM), permanent magnet (PMSFM) and combination of the two, called hybrid (HESFM). The maiden SFM was developed by combining the structures of Switched Reluctance Machine (SRM) and Permanent Magnet Synchronous Machine (SPMSM) was designed and developed in the mid-1950s as a single-phase flux switched flux switched alternator (Rauch et al. 1955, Shen et al. 2013, Faisal et al. 2016, Mahyuzie et al. 2016).

SFM is a doubly salient pole machine for various applications. Both WFSFM and HESFM require external circuit connections and have inherit high winding loss but PMSFM eliminates external circuit connections (Wang et al. 2010, Wei et al. 2009, Raminosoa et al. 2011). As a result, PMSFM has attracted so much interest due to its advantages of loss-free excitation and elimination of external circuit connection, because it records less copper loss. PMSFM has various factors including advances in magnetic material, and computer aided design tools (Fei et al. 2009, Enwelum and Erwan, 2017).

With PM being the natural source of flux, various topologies have been designed for numerous allied purposes namely; automotive and aerospace. Meanwhile, all these designs have inner rotor structure for out-wheel applications (Ahmad et al. 2012). Already, outer rotor PMSFM motor had been proposed for in-wheel application (Fei et al. 2009).

Meanwhile, all the designs mentioned above have been in salient rotor pole (Zulu et al. 2010). Figure 1 illustrates conventional SFMs is outer salient rotor. In Figure 1 (a), the conventional PMSFM consists of partitioned stator segments with PM sandwiched between stator teeth. It has complex structure and embracing all stator teeth winding, utilized high copper conductor. However, HESFM, has complex stator structure and embracing overlapping winding which leads to high material usage and resulting in high copper loss. Furthermore, it also requires a secondary excitation source [Ahmad et al. 2010).

In order to overcome high iron and copper losses associated with the conventional SFMs, this paper, has presented PMSFM using unconventional rotor segment (Enwelum and Erwan, 2017). A research that had been carried out showed using segmented rotor generated high torque (Mecrow and Zulu et al. 2010). The use of segmented rotor in flux switching mechanism has the benefit of operating with a bipolar flux in the magnetic circuit as bipolar flux linkage is achieved by the rotor from the armature winding (Zulu et al. 2010).

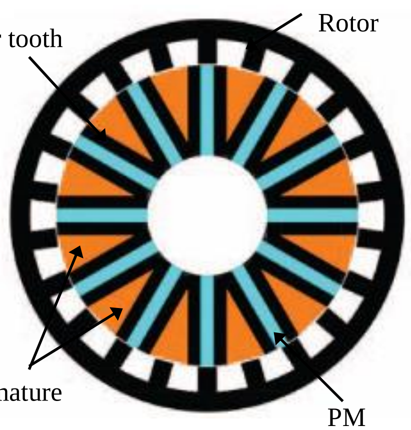

(a)

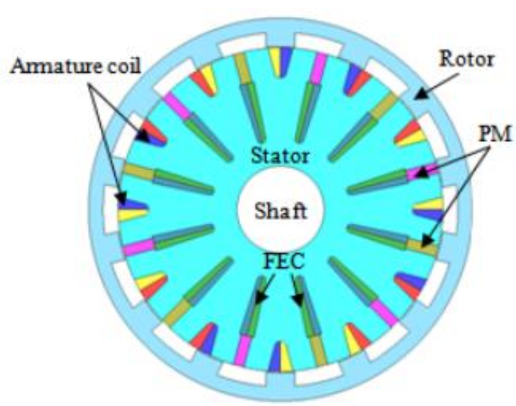

(b)

Figure 1 Conventional SFMs in outer rotor
(a) PMSFM (b) HESFM

2. METHODOLOGY AND ANALYSIS

The design specifications, parameter restrictions and electrical supply are summarized in (Enwelum and Erwan, 2017). Accordingly, specifications of the proposed motor in outer rotor structure have been chosen based on the surface permanent magnet synchronous motor (SPMSM) installed in eclimo electric scooter Model ES 11, with torque and power performances of 110Nm and 6000W. The dimensions are kept fixed as conventional, except that PM weight is reduced from 1.2kg to 1.0kg. Furthermore, external rotor shaft was utilized to retain the segments in order to be used for speed operation. Therefore, target torque and power are 352Nm and 36kW, far higher than conventional motor. Figure 2 illustrates the PMSFM under consideration in which the magnet flux and coil are in parallel and the variation of flux density in the magnets is rather very small.

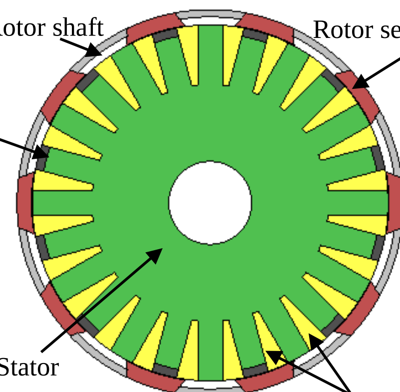

Figure 2 Cross-sections of proposed 24/10 stator-rotor segmented outer rotor PMSFM

Meanwhile, due to variation of flux density in the magnets, stator permanent magnets could be expressed as the equivalent magnetomotive force, MMF such that

$$F_{pm} = \frac{B_r}{\mu_r \mu_0} h_{pm} \tag{1}$$

and permeance $\Lambda_{pm} = \mu_r \mu_0 \frac{l_{pm} i_a}{h_{pm}}$ (2)

where h_{pm} and l_{pm} are the permanent magnet dimensions, and B_r is the remanence, this is the magnetization left behind in the stator core after external magnetic field has been removed.

In the same pattern, each stator slot experienced the net MMF F_f and is given by:

$$F_f = (I_1 - I_2)N_a \quad (3)$$

where I_1 and I_2 are phase currents, N_a is the number of turns per coil.

2.1 Cogging Torque Analysis

Cogging torque which is not desirable for machine operation arises from the interaction between the magnet in the stator and winding with the rotor. In the segmented rotor motor understudy, its cogging torque can be calculated based on energy method:

$$T_{cogging}(\theta) = -\frac{\partial W(\theta)}{\partial \theta} \quad (4)$$

where θ is rotor's angular position, W is the motor magnetic energy as in (Wei et al.2012).
Thus,

$$W(\theta) = \frac{1}{2\mu}\int_v B^2 dV \quad (5)$$

where B is magnetic flux density in all parts of motor including iron, μ is the permeability.

Meanwhile, the air-gap field distribution can be predicted from the product of air-gap flux density and air-gap relative permeance as in (Zhu et al. 2009),

$$B = G(\sigma, z)B(\sigma, \theta) \quad (6)$$

where $G(\sigma, z)$ is air-gap relative permeance and $B(\sigma, \theta)$ is air-gap flux density. Therefore, (5) can be expressed as in (Sang-Moon et al. 2001):

$$W(\theta) = \frac{1}{4\mu_0}(R_{rp}^{\ 2} - R_{sp}^{\ 2})\int_0^{l_{eff}}\int_0^{2\pi} G^2(\sigma, z)B^2(\sigma, \theta)d\sigma dz \quad (7)$$

where μ_0 is permeability of air, R_{rp}, R_{sp} are outer radius of rotor and inner radius stator, σ is angle along the circumference and l_{eff} is the effective stack length of motor.

2.2 Modelling of Motor

The proposed three-phase segmented rotor PMSFM shown under d-q axes consideration in figure 3 is modelled in terms of flux linkage which changes with rotor position, three-phase PM flux linkages uvw, ψ_{mu}, ψ_{mv} and ψ_{mw} are given as in (Hongyun et al. 2008)

$$\psi_{uvw} = \begin{bmatrix} \psi_{mu} = \psi_m \cos(p\theta_r) \\ \psi_{mv} = \psi_m \cos(p\theta_r - 120°) \\ \psi_{mw} = \psi_m \cos(p\theta_r + 120°) \end{bmatrix} \quad (8)$$

where ψ_m is the magnitude of the fundamental component, p is the number of rotor pole while θ_r is rotor position.

The armature inductances for 24/10 stator- rotor PMSFM, based on 2D-FEA: Self-inductance results for the 3Φ are given as:

$$\begin{bmatrix} L_{uu} = L_o - L_m\cos(p\theta_r) \\ L_{vv} = L_o - L_m\cos(p\theta_r + 120°) \\ L_{ww} = L_o - L_m\cos(p\theta_r - 120°) \end{bmatrix} \quad (9)$$

where L_o is the component of self- inductance and L_m is the magnitude of fundamental part while mutual-inductances are expressed as:

$$\begin{bmatrix} M_{uv} = M_{vu} = M_o - M_m\cos(p\theta_r - 120°) \\ M_{vw} = M_{wv} = M_o - M_m\cos(p\theta_r) \\ M_{wu} = M_{uw} = M_o - M_m\cos(p\theta_r + 120°) \end{bmatrix} \quad (10)$$

where M_o is the component of mutual inductance and M_m is the magnitude of fundamental part.

The components of transformation from stator to synchronous reference frame, the d- axis and q-axis of PMSFM understudy are classified in figure 3.

The rotor position, quadrature axis is chosen at the position A1 where the PM flux linkage is at peak level, and the *q*-axis is counter-clockwise. The 24/10 stator-rotor PMSFM, displacement between the axes, is 9° (mechanical degrees). Furthermore, stator to flux orientation based on synchronous rotor frame of reference, the three-phase stator to rotor Park's transformation by matrix is given in (11):

$$P = \frac{2}{3}\begin{bmatrix} \cos\theta_c & \cos(\theta_c - 120°) & \cos(\theta_c + 120°) \\ -\sin\theta_c & -\sin(\theta_c - 120°) & -\sin(\theta_c + 120) \\ \frac{1}{2} & \frac{1}{2} & \frac{1}{2} \end{bmatrix} \quad (11)$$

where θ_c is the rotor position between the coil A1 and the direct axis $p\theta_r$.

More so, combining (8) and (10), PM flux linkages in the rotor reference frame is transformed as:

$$\begin{bmatrix} \psi_{md} = \psi_m \\ \psi_{mq} = 0 \end{bmatrix} \quad (12)$$

Equation (12) depicts that the transformed d-axis PM flux linkage are equal and also the linkage in q-axis is zero (0). Obviously, transformed three-phase inductance component in rotor frame is given as stated in (13):

$$\begin{bmatrix} L_d = L_o - M_o - \frac{3}{2}L_m \\ L_q = L_o - M_o + \frac{3}{2}L_m \\ L_o = L_{dq} = L_{qd} = L_{d0} = 0 \end{bmatrix} \quad (13)$$

$$\begin{bmatrix} L_o - M_o = \frac{1}{2}(L_d + L_q) \\ L_m = \frac{L_d - L_q}{3} \end{bmatrix} \quad (14)$$

where $L_d, L_q, L_o, L_{dq}, L_{qd}$ are inductance components transformed in rotor reference frame.

Therefore, sum of d-axis and q-axis flux linkages expression confirm the equation stated:

$$\begin{bmatrix} \psi_d = L_d i_d = \psi_m + (L_o - M_o - \frac{3}{2}L_m)i_d \\ \psi_q = L_q i_q = (L_o - M_o - \frac{3}{2}L_m)i_q \end{bmatrix} \quad (15)$$

Furthermore, the *d*-axis and *q*-axis voltage equations are expressed, is obtained as:

$$\begin{bmatrix} V_d = \frac{\partial \psi_d}{\partial t} - \omega_c \psi_q + R_c i_d = -p_r \omega_r L_q i_q + R_c i_d \\ V_q = \frac{\partial \psi_q}{\partial t} + \omega_c \psi_d = p_r \omega_r \psi_m + p_r \omega_r L_d i_d + R_c i_d \end{bmatrix} \quad (16)$$

where R_c is the reactance of the winding coil and p_r is the rotor pole number.

More so, frequency of inverter is linked to rotor's speed, thus, given as

$$\omega_c = p\omega_r \quad (17)$$

where ω_c is the frequency of inverter and ω_r is rotor's speed

The electromagnetic torque T_{em}, is derived expressly as

$$T_{em} = \frac{3}{2}p_r\left[\psi_m i_q + (L_d - L_q)i_d i_q\right] \quad (18)$$

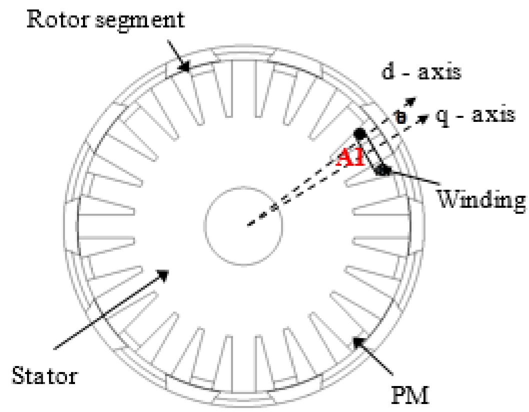

Figure 3 Considerations of *d* and *q* axes of motor

3. RESULTS AND DISSCUSSION

3.1 Open-Circuit Field Distribution

The field distribution of proposed outer rotor motor under no-load condition is shown in figure 4 in which flux linking coil A1 varies from medium to maximum in the first quadrant as rotor rotates and to zero and this changes polarity and magnitude at the fourth quadrant as in figure 4(a) to (b). Meanwhile, maximum flux linkage is determined by the proportion in the magnetic circuit with respect to the axis of coil in reference, as the segmented rotor is aligned with stator tooth on the side of magnet as in Figure 4(a).

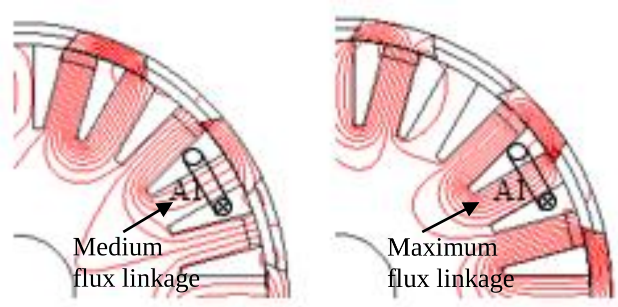

(a) (b)

Figure 4 Open circuit field distribution at minimum and maximum flux linkage with coil phase A1

3.2 Flux Linkage and Induced EMF

Figure 5 presents proposed PMSFM using unconventional rotor segment for in-wheel application whose flux linkage and induced EMF are depicted with coil phase A1. Meanwhile, segmented rotor pole structure using permanent magnet excitation permits the use of alternate tooth winding, utilizing less copper material, enables short flux path, these result in high flux linkage and yielding to higher torque [2]. Various other advantages include improvement of slot area where electric loading is fixed. More importantly, segmented rotor motors are capable of fault tolerant, a property to remain working in case of system fault. The presence of harmonics resulted from design disorder which will be improved during optimisation.

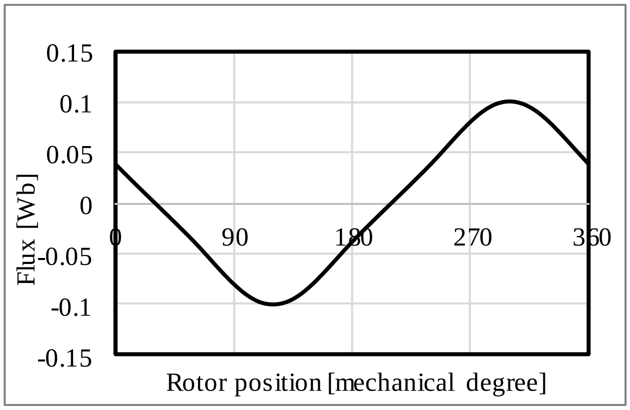

(a)

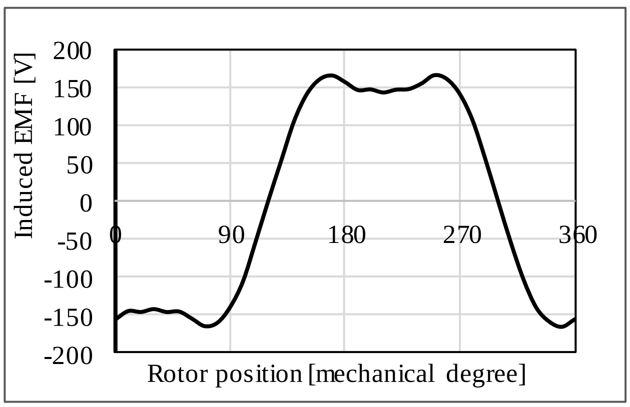

(b)

Figure 5 Flux linkage and induced EMF waveforms of proposed PMSFM at phase coil A1

3.3 Torque and Current Characteristics of PMSFM

The torque generated by current fed into motor understudy has been analysed using JMAG simulation tool version 14 and the result is presented in figure 6. The maximum current density is *Ja* 30 A/mm2. As seen, it is clear that PMSFM exhibited higher increase in torque output at low current density compared to increased current value. However, it is obvious that proposed motor increases torque generation with increase in current density, though it is not linear from *Ja* 15 A/mm2

3.4 Torque and Power Characteristics of PMSFM

Figure 7 illustrates motor's torque and power characteristics performance under load condition. From the plot, it is seen that power profile is constant throughout torque regions. Meanwhile, maximum torque of the proposed PMSFM is 352Nm and power out of 36kW. This performance shows that proposed motor is high torque, low speed and constant power application.

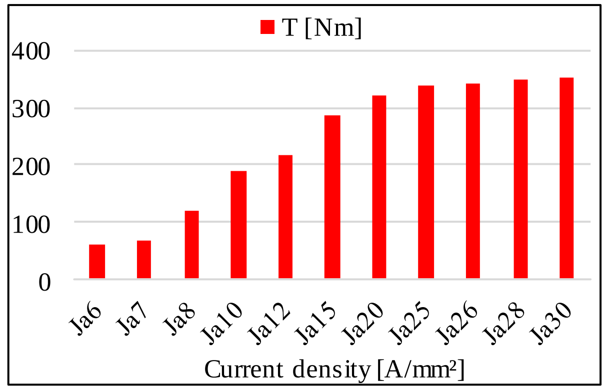

Figure 6 Torque and current density of Performance of PMSFM

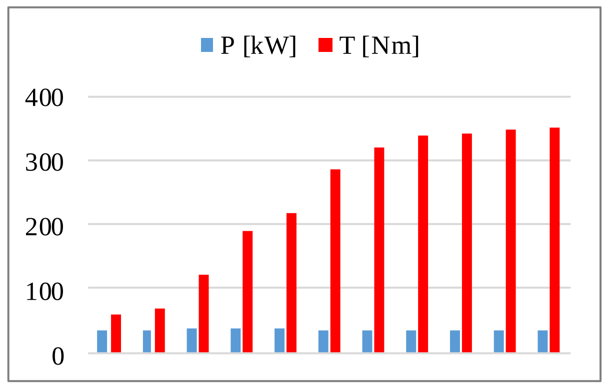

Figure 7 Torque and power performance

4. CONCLUSION

This paper has designed and presented permanent magnet switched flux motor employing segmented rotor suitable for in-wheel and fuel independent vehicle application. Combustion engine in which fossil oil must be fired in its chamber has been expensive in addition to manufacturing complexities. Moreover, fossil oil is getting depleted, the urgent need for transition. The motor consisted 24/10 stator-rotor segmented and having an external rotor shaft for retainment. The 2-D FEA was by JMAG Designer tool to investigate performances in terms of cogging torque analysis, induced EMF and output torque. Result of motor performance achieved higher torque value for heavy weight applications. High torque is crucially significance as inertia overcomer and acceleration sustainer projected it as viable candidate for electric vehicles powered by stored electricity.

REFERENCES

Ahmad, M. Z., Erwan, S., Haron, Z. A., Haron And Kosaka, T. 2012. Preliminary Studies On A New Outer Rotor Permanent Magnet Flux Switching Machine With Hybrid Excitation Flux For Direct-Drive EV Application, IEEE International Conference on Power and Energy, 928-933.

Byeong-Mun, C., Ki-Chan C and Jang-Young C. 2010. Design Of An Outer-Rotor-Type Permanent Magnet Rotor For Electric Scooter Propulsion Systems, International Power Electronics Conference, 2736-2742.

Chen, J. T., and Zhu Z. Q. 2010. Winding Configuration And Optimal Stator And Rotor Pole Combination Of Flux-Switching PM Brushless AC Machines, IEEE Trans. Energy Conversion, (25) 2: 293–302.

Enwelum, I. M., Erwan S and Faisal Khan. 2018. Consideration Of Permanent Magnet Flux Switching Motor In Segmented Rotor For In-Wheel Vehicle Propulsion, International Conference on Computing, Mathematics and Engineering Technologies (iCoMET), 1-6.

Enwelum I. M and Erwan S. 2017. Flux Switching Permanent Magnet Motor Using Segmented Outer Rotor Structure For Electric Scooter, Indonesian Journal of Electrical Engineering and Computer Science (IJEECS), 6: 379-386.

Faisal, K., Erwan S and Ahmad M.Z. 2016. Review Of Witched Flux Wound Field Machines Technology, IETE Technical Review (http://dx.doi.org/10.1080/02564602.)

Fei, W., Luk P. C. K., Shen J. X. S., Wang Y. and Jin M. 2009. A Novel Outer-Rotor Permanent Magnet Flux Switching Machine For Urban Electric Vehicle Applications, in Proc. 3rd Inter. Conference Power Elect. Systems Applications, 1-6.

Galea, M., Gerada C and Hamiti T. 2012. Design Considerations For An Outer Rotor, Field Wound Flux Switching Machine, International Conference of Electrical Machines, ICEM, 171-176.

Hoang, E., Ben-Ahmed A. H and Lucidarme J. 1997. Switching Flux PM Polyphase Synchronous Machines, In Proc. 7th European Conf., on Power Electrons Application, 3, 903–908.

Hongyun, J., Cheng M., Hia W and Fu X. 2008. Investigation And Implementation Of Control Strategies For Flux-Switching Permanent Magnet Motor Drives, IEEE, Industry Applications Society Annual Meeting

Hwang, S.M., Eom J.B., Hwang G. B., Jeong W.B and Jung Y. H. 2000. Cogging Torque And Acoustic Noise Reduction In Permanent Magnet Motors By Teeth Pairing, IEEE Transaction on Magnetics.

Jin, M. J., Wang C. F., Shen J. X and Xia B. 2009. A Modular PM Flux Switching Linear Machine With Fault-Tolerant Capability, IEEE Transactions on Magnetics, (45)8: 3179–3186.

Kun, X., Xinhua M., Xiaojiang W., Hong Y and Gangyi H. 2018, A New Type Of CPPM Machine With Stator Axial Magnetic Ring, Journal of Electrical Engineering, (13)3:1285-1293.

Liang, X and Luy Y. 2006. Harmonics Analysis In Induction Motors, Conference on Electrical and Computer Engineering, (CCECE)

Liu, H., Wang Y., Deng Z.Q., Song L.C. 2014. Comparative Study Of The Parallel Hybrid Excited Flux Switching Machine Topology For Aerospace Generator System," IEEE Conference and Expo on Transportation Electrification Asia-Pacific, 1-6.

Mahyuzie, J., Erwan S., and Rajesh K. 2016. A New Switched Flux Machine Employing Alternate Circumferential And Radial (AlCiRaF) Permanent Magnet For Light Weight EV. Journal of Magnetics, (21)4:537-543

Mecrow, B. C., Bedford T. J., Bennet J. W and T. Celik. 2006. The Use Of Segmental Rotors For 2-Phase Flux Switching Motors, Proc. 17th International Conference on Electrical Machines, ICEM, 608.

Min, W., Chen J. T., Zhu Z. Q., Y. Zhu Y., Zhang M and Duan G. H. 2011. Optimization And Comparison Of Novel E-Core And C-Core Linear Switched Flux PM Machines, IEEE Transactions on Magnetism, (47)8: 2134–2141.

Noman, U., Faisal K., Wasiq U Abdul B., Muhammad U and Zeeshan K. 2018., Analytical Modeling Of Open-Circuit Flux Linkage, Cogging Torque And Electromagnetic Torque For Design Of Switched Flux Permanent Magnet Machine", Journal of Magnetics, (23)2: 253-266.

Owen, R. L., Zhu Z. Q., Thomas A. S., Jewell G. W and Howe D. 2010. Alternate Poles Wound Flux Switching Permanent Magnet Brushless AC Machines. IEEE Transactions Industry Applications, (46)2: 790–797.

Raminosoa, T., Gerada C and Galea M. 2011. Design Considerations For A Fault Tolerant Flux Switching Permanent Magnet Machine, IEEE Transactions Industrial Electronics., (58): 2818-2825.

Rauch, S. E and Johnson L. J, "Design Principles of Flux Switch Alternator, Transaction Of American Institute Of Electrical Engineers, Part III: Power System Apparatus, (74)3:1261-1268, 1955.

Shen, J. S and Fei W. Z. 2013. Permanent Magnet Flux Switching Machine Topologies, Analysis And Optimisation, 4th International Conference on Power Engineering, Energy and Electric Drives.

Tang, T., Motoasca T. E., Paulides J. J. H and Lomonova E. A. 2012. Analytical Modeling Of Flux Switching Machines Using Variable Global Reluctance Networks, Proceedings, 20th International Conference on Electrical Machines (ICEM), 2792-2798.

Walker, C.S, Polinder H and Ferreira J. A. 2013. High Torque Density High Efficiency Flux Switching Machine For Aerospace Application, IEEE Journal of Emerging and Selected Topics in Power Electronics, (1):327-336.

Wang, Y., Jin M. J., Shen X. J.,Fei W.Z and Luk P.C.K, 2010. An Outer Rotor Flux Switching Machine For Traction Applications, IEEE Energy Conversion Congress and Exposition, 1723-1730.

Wei, X., Gang L., Tianshi W., Xinghuo Y., Jianguo Z and Youguang G. 2012. Theoretical Research On New Laminated Structure Flux Switching Permanent Magnet Machine For Novel Topologic Plug-In Hybrid Electrical Vehicle. IEEE Transactions on Magnetics, (48)11: 4050-4053.

Zang, H., Hee-lee D, Woo lee C and Woo-ann J. 2014. Design And Analysis Of Synchronous Motor Employing A Segmental Rotor Type 12/8 Switched Reluctance Motor, Journal of Power Electronics. (14):866-873.

Zhu, L., Jiang Z. Q., and Chan. 2009. Analytical Methods For Minimizing Cogging Torque In Permanent Magnet Machines, IEEE Transactions on Magnetics (45)4: 2023-2031.

Zulu, A., Mecrow B. C and Armstrong M., Topologies For Wound Field Three-Phase Segmented Rotor Flux Switching Machines, In Power Electronics, Machines and Drives (PEMD), 5th Inter., Conference, 1-6, 2010.